New results on the spin-dependent structure function of the deuteron, g_1^d

Helena Santos
on behalf of the COMPASS Collaboration

LIP - Laboratório de Instrumentação e Física Experimental de Partículas, Av. Elias Garcia 14, 1000-149 Lisbon, Portugal

The COMPASS experiment at the CERN SPS has an extensive program focused on the nucleon structure and on hadron spectroscopy. A main topic of investigation is the spin dependent structure function g_1^d of the deuteron. Results obtained in the kinematic ranges $Q^2 < 1\,(\mathrm{GeV/c})^2$ and $0.0005 < x < 0.02$, as well as $1 < Q^2 < 100\,(\mathrm{GeV/c})^2$ and $0.004 < x < 0.7$ are presented. The results of a global QCD fit at NLO to the world g_1 data are discussed.

PACS: 13.60.Hb; 13.88.+e; 24.85.+p
Key words: Deep inelastic scattering; nucleon spin; A_1^d asymmetry; g_1^d structure function; QCD analysis

1 Introduction

The history of the spin structure of the nucleon begun more than 30 years ago with polarised deep inelastic scattering measurements at SLAC [1]. At that time the quark-parton model has predicted that 60 % of the nucleon spin was entirely given by the u and d quarks [2], which validity has been supported by the poor x range of the experiment ($x > 0.1$). Then the EMC Collaboration extendend the measurements to $x > 0.01$ and came out with the unexpected value of $0.12 \pm 0.09 \pm 0.14$ [3]. Such a result motivated a set of experiments covering different x ranges at CERN [4], SLAC [5–8], DESY [9] and JLAB [10]. All these experiments confirmed the small contribution of the quarks (about 20–30 %), and thus more contributions were necessary. For a nucleon with $+1/2$ helicity one should have the sum rule:

$$S_n = \frac{1}{2} = \frac{1}{2}\Delta\Sigma + \Delta G + L_q + L_G \tag{1}$$

where $\Delta\Sigma$ stands for the contribution from the quarks ($\Delta\Sigma = \Delta u + \Delta d + \Delta s$), ΔG is the contribution of the gluons and $L_{q,G}$ are their angular orbital momenta. In order to obtain a complete picture of the nucleon the transverse spin distributions of the quarks, $\Delta_T q(x)$, are also needed.

The main topic of investigation at COMPASS is the measurement of ΔG [11]. However, the experimental program is very wide; all, but $L_{q,G}$ contributions, can be studied at COMPASS with unprecedented precision. This article reports the experimental procedure to measure the spin-dependent structure function, g_1, and how the evaluation of its first moment leads to the first term of equation 1. Also a NLO QCD analysis performed in order to obtain an indirect measurement of ΔG is described.

2 Experimental procedure

COMPASS makes use of the SPS facilities, impinging a high intensity 160 GeV/c muon beam on a ^{6}LiD polarised target. Besides the scattered muon, other particles produced in deep inelastic scattering are detected in a two-stage spectrometer. Data presented in this article have been collected in the years 2002, 2003 and 2004, corresponding to an integrated luminosity of about 2 fb^{-1}.

Muons originate from pion and kaon decays produced by the proton beam colliding on a beryllium target. In such decay mechanism muons become longitudinally polarised. The target consists in two 60 cm long cells, with 3 cm diameter and separated by 10 cm. They are located inside a superconducting solenoid magnet that provides a field of 2.5 T along the beam direction. The maximum angle of aperture of the magnet is 70 mrad [1]). The two cells are oppositely polarised by dynamic nuclear polarisation (DNP), so that the deuteron spins are parallel ($\uparrow\uparrow$) or antiparallel ($\uparrow\downarrow$) to the spins of the incoming muons. The polarisations of the two cells are inverted every 8 hours by rotating the magnetic field direction. In this way acceptances do cancel out in the asymmetry calculation, providing that the acceptance ratios remain unchanged after field rotation, i.e., if $a_1/a_2 = a_1'/a_2'$. Eventual systematic effects related to the magnetic field do cancel out as well, by reversing the polarisation of each target cell, by DNP, at least once per running period.

The two spectrometers (Large Angle Spectrometer (LAS) and Small Angle Spectrometer (SAS)) are located around two dipole magnets, the so-called SM1 and SM2, supplying field integrals of 1 and 4.4 Tm, respectively. Scintillating fibres and silicon detectors ensure tracking in the beam region, complemented by MicroMeGas and GEM detectors up to 20 cm from the beam. Drift chambers, multi-wire proportional chambers and straw tubes cover both LAS and SAS spectrometers. Iarocci-type and drift tubes track the muons downstream of the two hadron absorbers, located in each sector. Electromagnetic and hadronic calorimeters are integrated in both spectrometers. A sophisticated Ring Imaging Čerenkov Detector separates kaons from pions with momentum up to 43 GeV/c [2]). The detailed description of the spectrometer can be found at Ref. [12].

The COMPASS data acquisition system is triggered by coincidence signals in hodoscopes. Inclusive triggers require the detection of the scattered muon, while semi-inclusive triggers are based on the muon energy loss and on the presence of a hadron signal in the calorimeters. Purely calorimetric triggers are based on the energy deposit in the hadron calorimeter without any condition on the scattered muon. Triggers due to halo muons are eliminated by veto counters installed upstream from the target.

DIS events are selected by cuts on the four-momentum transfer squared ($Q^2 > 1\,(\mathrm{GeV/c})^2$) and the fractional energy of the virtual photon ($0.1 < y < 0.9$). Such a kinematic window allows a wide Bjorken scaling variable interval, $0.004 < x < 0.7$. Furthermore, strict quality criteria are applied to data ensuring that events

[1]) From the run of 2006 on, COMPASS has a new magnet providing an acceptance a factor 2.5 higher.

[2]) This detector has not been used in the presented analysis.

originate in the target, preventing fake triggers and demanding equal muon fluxes on the two target cells. After data selection 89×10^6 events are available for analysis. Fig. 1 shows the fraction distributions of the different triggers. Inclusive ones cover the full range of x and are dominant in the medium (x, Q^2) region. Semi-inclusive triggers contribute mainly at low x and low Q^2, while the pure calorimetric triggers contribute mainly to large Q^2.

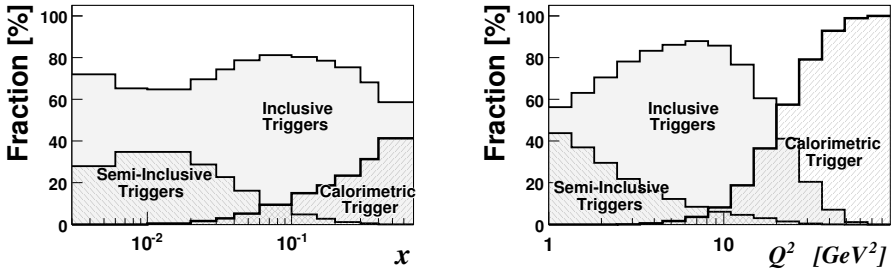

Fig. 1. Fraction of inclusive, semi-inclusive, and calorimetric triggers as a function of x (left) and Q^2 (right).

In order to have access to the spin-dependent structure function, g_1^d, the longitudinal photon-deuteron asymmetry, A_1^d, has to be evaluated. In the framework of the quark parton model this quantity can be directly related to the quarks polarisation via

$$A_1 = \frac{(\sigma_{\gamma\mu}^{\uparrow\downarrow} - \sigma_{\gamma\mu}^{\uparrow\uparrow})}{(\sigma_{\gamma\mu}^{\uparrow\downarrow} + \sigma_{\gamma\mu}^{\uparrow\uparrow})} \simeq \frac{\sum_q e_q^2(\Delta q + \Delta\bar{q})}{\sum_q e_q^2(q + \bar{q})}\,. \tag{2}$$

The experimental asymmetry, A_μ^d, relates to A_1^d by means of:

$$A_\mu^d = D(A_1^d + \eta A_2^d)\,, \tag{3}$$

where D and η depend on kinematics. The transverse asymmetry A_2^d has been measured at SLAC and found to be small [13], so, in practice we are left only with the first term, $A_1^d \simeq A_\mu^d / D$. The virtual-photon depolarisation factor D depends on the ratio of longitudinal and transverse photo-absorption cross sections $R = \sigma^L/\sigma^T$. The experimental asymmetry A_μ^d is given by

$$A_\mu^d = \frac{1}{P_{\rm B} P_{\rm T} f} \frac{1}{2} \Big[\frac{N^{\uparrow\downarrow} - N^{\uparrow\uparrow}}{N^{\uparrow\downarrow} + N^{\uparrow\uparrow}} + \frac{N'^{\uparrow\downarrow} - N'^{\uparrow\uparrow}}{N'^{\uparrow\downarrow} + N'^{\uparrow\uparrow}} \Big], \tag{4}$$

where N stands for the number of detected events in each target cell, N' is the corresponding number after magnetic field reversal, $P_{\rm B}$ and $P_{\rm T}$ are the beam and target polarisations, respectively, and f is the dilution factor, which accounts for the ratio of the photon-absorption cross-sections on the deuteron and on all nuclei that fill the target cells. Fig. 2 (top left) shows the beam polarisation as a function of the beam momentum. The average has been –80 % for the 2004 run and –76 % for

the 2002 and 2003 ones. The momentum of the incoming muon is centred around 160 GeV/c with an RMS of 8 GeV/c for the Gaussian core. In the present analysis its value is required to be between 140 and 180 GeV/c. The polarisation of the target cells is about 50 %, although the positive polarisation (nucleon spin along the magnetic field) is always larger in absolute values than the negative polarisation, as can be seen in Fig. 2 (top right). In the bottom left and bottom right of the same figure the depolarisation and dilution factors for the analysed x domain are shown. The dilution factor is ≈30–40 %, having different trends for the inclusive and hadron [3]) events. Such behaviour occurs at large x due to the different kinematic conditions of the two classes of triggers and at low x because the elastic and quasi-elastic cross-section contributions vanish in the hadron events case, increasing their dilution factor.

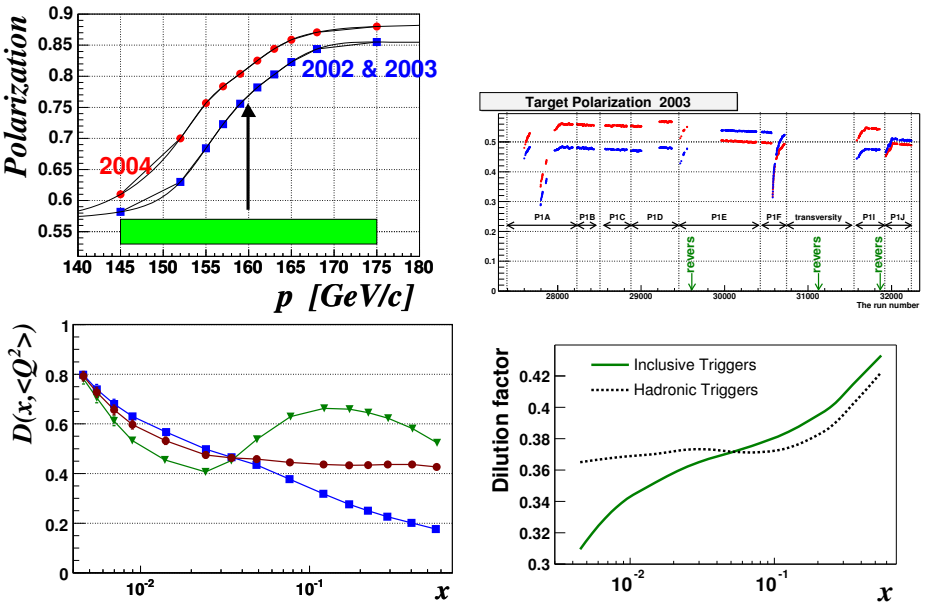

Fig. 2. Top: Beam polarisation as a function of the beam momentum (left); Target polarisation as a function of time (right); Bottom: Depolarisation factor (squares: inclusive events, triangles: hadron events, circles: average) (left) and dilution factor (right) as a function of x.

3 The A_1^d asymmetries

The starting point for the A_1^d asymmetry extraction is to count the events detected in each target cell, $N_i = a_i \phi_i n_i \sigma_0 (1 + P_B P_T f D A_1^d)$, where a_i is the accep-

[3]) events that have produced at least 1 hadron.

tance of the target cell i, ϕ_i is the incoming muon flux, n_i is the number of target nucleons and σ_0 is the unpolarised cross-section. The ratio $N_1 N_2' / N_2 N_1'$ relates to A_1^d through a second order equation, in which the fluxes ϕ_i cancel out by a proper cut on the data that ensures equal muon fluxes for both target cells. The ratio of acceptances do cancel out as well, if $a_1/a_2 = a_1'/a_2'$. This condition is expected to hold since the spins are reversed quite often. In order to minimize the statistical error of the asymmetry, each event is weighted by the product of its associated kinematic factors f, D and the beam polarisation. As the target polarisation is time dependent it is taken as the average value of the run, instead. The A_1^d asymmetry measurement is performed separately for inclusive and hadron triggers. Such a procedure is necessary because radiative corrections [14], although very small, are not the same for the two classes of events. Once the two asymmetries have been measured they are averaged in order to produce the final result, as their trends as a function of x are perfectly compatible within the statistical errors.

Fig. 3 reports A_1^d as a function of x for quasi-real photon interactions ($Q^2 < 1\,(\mathrm{GeV/c})^2$) using 2002 and 2003 data. 280 million events have been analysed corresponding to an integrated luminosity of $1.5\,\mathrm{fb}^{-1}$. One should bear in mind that, although part of the x domain ($0.0005 < x < 0.02$) is the same of the DIS events, this plot refers to completely different physics [15]. Apart from the different Q^2 and x domain, data selection is slightly different from the one performed for DIS events. The asymmetry is compatible with 0 over the whole x range. The error bars are statistical and the grey band corresponds to systematic errors, which are due to false asymmetries mainly. Details on this analysis can be found in [15].

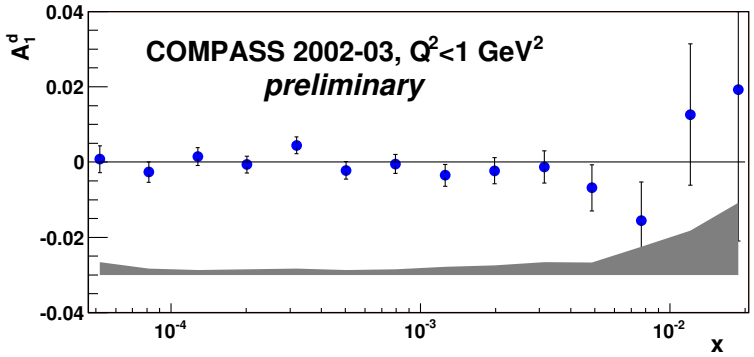

Fig. 3. The asymmetry $A_1^d(x)$ for quasi-real photons ($Q^2 < 1\,(\mathrm{GeV/c})^2$) as a function of x. Errors bars are statistical. Grey band shows the systematic errors.

Fig. 4 shows A_1^d as a function of x for DIS events ($Q^2 > 1\,(\mathrm{GeV/c})^2$), as measured by COMPASS using 2002, 2003 and 2004 data [18]. The results from the experiments SMC [4], E143 [6], E155 [8] and HERMES [19], are also shown. The asymmetry is 0 for $x < 0.05$ and becomes larger and larger as x increases, reaching 60 % at $x \simeq 0.7$. The agreement is very good among the different data sets. It

should be noted that at very low x only COMPASS and the precursor SMC were able to measure this asymmetry, the COMPASS results being essential to disentangle the A_1^d behaviour at $x < 0.03$. Error bars are statistical and the grey band corresponds to systematic errors on COMPASS measurements, whose sources come from the uncertainty on beam and target polarisations (5 %), dilution factor (6 %) and depolarisation factor (4–5 %). Radiative corrections and the neglection of A_2 are found to have a small effect. The upper limit for the systematic error due to false asymmetries is half of the statistical one.

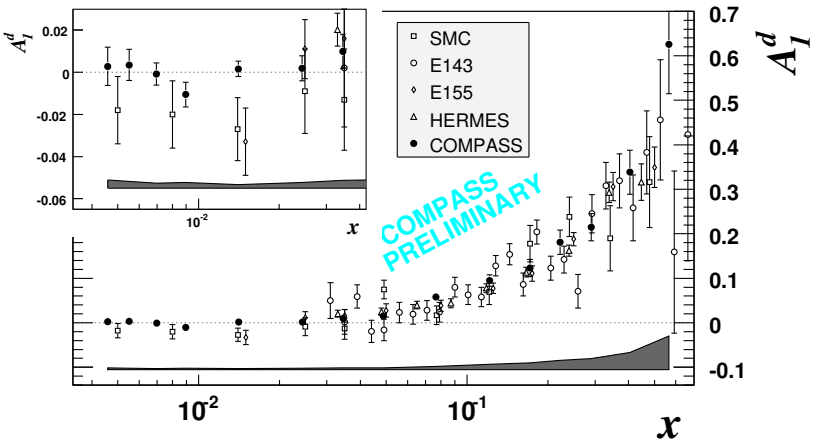

Fig. 4. The asymmetry $A_1^d(x)$ as measured by the world spin experiments. SLAC values of g_1/F_1 have been converted to A_1 and E155 data corresponding to the same x have been averaged over Q^2. The error bars are statistical. The shaded areas show the size of the COMPASS systematic errors; see text for details.

4 The g_1^N structure function

The spin-dependent structure function of the nucleon, $g_1(x)$, is obtained from $A_1(x)$ and the spin-independent structure function $F_2(x)$ through

$$g_1(x) = A_1(x)\frac{F_2(x)}{x(1+R)}\,. \tag{5}$$

Figure 5 shows g_1^d as a function of x for quasi-real photon interactions. g_1^d is found to be consistent with 0 in the investigated x range. The statistical precision of the COMPASS results [15] has improved considerably compared with SMC [16] and HERMES [17].

Figure 6 shows g_1^d, as a function of x for DIS events [18]. The SMC results [4] have been moved to the Q^2 of the corresponding COMPASS points. The two curves are the results of two QCD fits at NLO in the $\overline{\text{MS}}$ renormalisation and factorisation scheme. These fits require input parameterisations of the quark singlet spin

distribution $\Delta\Sigma(x)$, non-singlet distributions $\Delta q_3(x)$ and $\Delta q_8(x)$, and the gluon spin distribution $\Delta G(x)$, which evolve according to the DGLAP equations. They are written as:

$$\Delta F_k \;=\; \eta_k \frac{x^{\alpha_k}\,(1-x)^{\beta_k}\,(1+\gamma_k x)}{\int_0^1 x^{\alpha_k}\,(1-x)^{\beta_k}\,(1+\gamma_k x)dx}\,, \tag{6}$$

where ΔF_k represents each of the polarised parton distribution functions (PDF) and η_k is the integral of ΔF_k. The moments, η_k, of the non-singlet distributions Δq_3 and Δq_8 are fixed by the baryon decay constants (F+D) and (3F−D) respectively [20], assuming $\mathrm{SU}(3)_f$ flavour symmetry. The linear term γx is used only for the singlet distribution, in which case the exponent β_G is fixed because it is poorly constrained by the data. Thus, 10 parameters stand in input distributions. Data are well described by two solutions, $\Delta G > 0$ and $\Delta G < 0$.

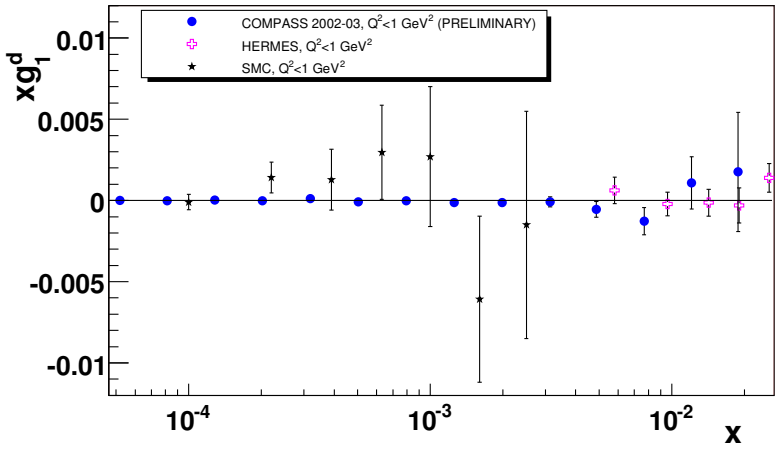

Fig. 5. The spin-dependent structure function of the deuteron, g_1^d, in the low x and low Q^2 region, as measured by COMPASS, SMC and HERMES.

Figure 7 shows the QCD fit to proton, deuteron and ^{3}He targets, which solution gives $\Delta G < 0$ (an indistinguishable curve is obtained for the solution $\Delta G > 0$). All data have been evolved to a common Q_0^2 by means of the $g_1(x, Q^2)$ fitted parameterisation,

$$g_1(x, Q_0^2) = g_1(x, Q^2) + \left[g_1^{fit}(x, Q_0^2) - g_1^{fit}(x, Q^2)\right]. \tag{7}$$

We have used several fits of g_1 from the Durham data base [21]: Blümlein–Böttcher [22], GRSV [23] and LSS05 [24]. The value $Q_0^2 = 3\,(\mathrm{GeV/c})^2$ as been chosen as reference because it is close to the average Q^2 of the COMPASS DIS data. The deuteron data are from Refs. [4, 6, 8, 19], the proton data from Refs. [4, 6, 19, 25, 26] and the ^{3}He data from Refs [10, 27, 28, 29]. In order to optimise the use of the COMPASS data in this fit, all bins, except the last one, have been subdivided

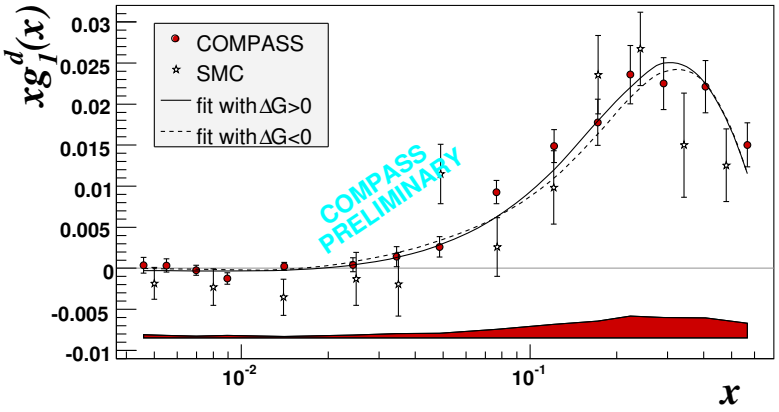

Fig. 6. The spin-dependent structure function of the deuteron, g_1^d, as a function of x ($Q^2 > 1\,(\mathrm{GeV/c})^2$). The COMPASS points are given at the $\langle Q^2 \rangle$ where they were measured. The SMC points have been moved to the Q^2 of the corresponding COMPASS points. Only statistical errors are shown. The shaded band at the bottom shows the COMPASS systematic error. The curves show the results of QCD fits with $\Delta G > 0$ and $\Delta G < 0$.

into three Q^2 intervals. The number of COMPASS data points used in the fit to deuteron data is thus 43, out of a total of 230. The resulting values of $g_1(x, Q^2)$ are calculated for the (x_i, Q_i^2) of each data point and compared to the experimental values. The parameters are found by minimizing the sum

$$\chi^2 = \sum_{i=1}^{N=230} \frac{\left[g_1^{fit}(x_i, Q_i^2) - g_1^{exp}(x_i, Q_i^2)\right]^2}{\left[\sigma(x_i, Q_i^2)\right]^2}. \tag{8}$$

where $\sigma(x_i, Q_i^2)$ are the statistical errors for all data sets, except for the proton data of E155 where the uncorrelated part of the systematic error on each point is added in quadrature to the statistical one. In order to keep the parameters in their physical range, the polarised strange sea distribution $\Delta s(x) + \Delta\overline{s}(x) = (1/3)(\Delta\Sigma(x) - \Delta q_8(x))$ is calculated at every step and required to satisfy the positivity condition $|\Delta s(x)| \leq s(x)$ at all Q^2 values. The same constraint is imposed to the gluon spin distribution $\Delta G(x)$. The unpolarised distributions $s(x)$ and $G(x)$ are taken from the MRST parameterisation [30]. Two different programs have been used to fit the data – one uses the DGLAP evolution equations for the spin structure functions [31], the other uses the evolution of moments [32]. Both programs give consistent values of the fitted PDF parameters and similar χ^2-probabilities.

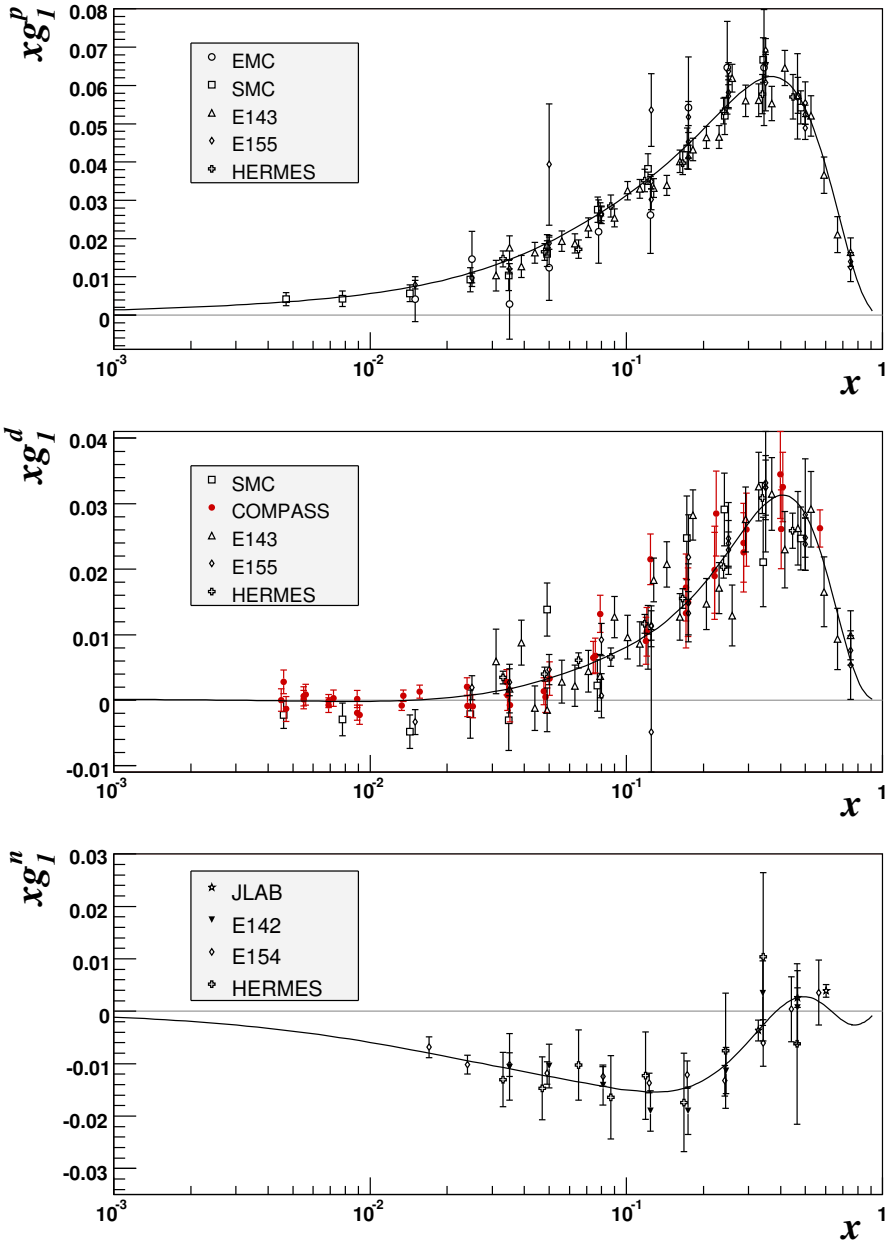

Fig. 7. The world data and QCD fit at $Q^2 = 3\,(\mathrm{GeV/c})^2$, obtained with the program of Ref. [31]. The curve corresponds to the solution with $\Delta G < 0$.

The polarised parton distributions for the three flavours and ΔG are shown in Fig. 8 for both $\Delta G < 0$ and $\Delta G > 0$ solutions. Quark distributions are weak dependent on the sign of ΔG.

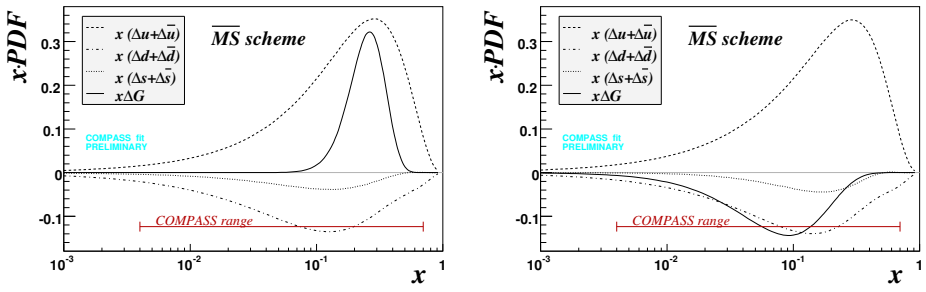

Fig. 8. Distributions $x(\Delta u + \Delta\bar{u})$, $x(\Delta d + \Delta\bar{d})$, $x(\Delta s + \Delta\bar{s})$ and $x\Delta G$ corresponding to the fits with $\Delta G > 0$ (*left*) and $\Delta G < 0$ (*right*) at $\mathrm{Q}^2 = 3\ (\mathrm{GeV/c})^2$.

Previous QCD fits, not including COMPASS data, found a positive $\Delta G(x)$ and gave a sharp decrease of $g_1^d(x)$ for $x \lesssim 0.025$ at $Q^2 = 3\,(\mathrm{GeV/c})^2$, as shown by the dotted line of Fig. 9. Indeed, taking into account the COMPASS data, there is no evidence for a decrease of the structure function in the limit $x \to 0$. The data are still compatible with a positive ΔG, as shown by the full line in Fig. 9, however a dip appears at $x \simeq 0.25$, which is related to the shape of the fitted $\Delta G(x)$ – in order to avoid pushing g_1^d down to negative values, the gluon spin distribution must be close to zero at low x, and it is also strongly limited at large x by the positivity constraint $|\Delta G(x)| < G(x)$. The whole distribution is thus squeezed in a narrow interval. On the contrary, the fit with negative ΔG reproduces very well the COMPASS low x data with a much smoother distribution of $\Delta G(x)$ (dashed line on Fig. 9) and without approaching the positivity limit. In this plot g_1^N is related to the measured g_1^d by correcting it for the D-wave state probability of the deuteron, $g_1^N = g_1^d/(1 - 1.5\omega_D)$, with $\omega_D = 0.05 \pm 0.01$ [33].
Although the shapes of the gluon distribution differ over the whole x range, the fitted values of η_G are small and similar in absolute value $|\eta_G| \approx 0.2$–0.3. Similarly η_Σ reveals weak dependence on the shape of ΔG, being slightly larger in the fit with $\Delta G < 0$. Such a feature is not surprising since in this case $\Delta\Sigma(x)$ remains positive over the full range of x:

$$\eta_\Sigma\left(Q^2 = 3\,(\mathrm{GeV/c})^2\right) = 0.28 \pm 0.01(\mathrm{stat.})(\Delta G > 0)\,, \tag{9}$$

$$\eta_\Sigma\left(Q^2 = 3\,(\mathrm{GeV/c})^2\right) = 0.32 \pm 0.01(\mathrm{stat.})(\Delta G < 0)\,. \tag{10}$$

The singlet moment derived from the fits to all g_1 data is thus:

$$\eta_\Sigma\left(Q^2 = 3\,(\mathrm{GeV/c})^2\right) = 0.30 \pm 0.01(\mathrm{stat.}) \pm 0.02(\mathrm{evol.})\,. \tag{11}$$

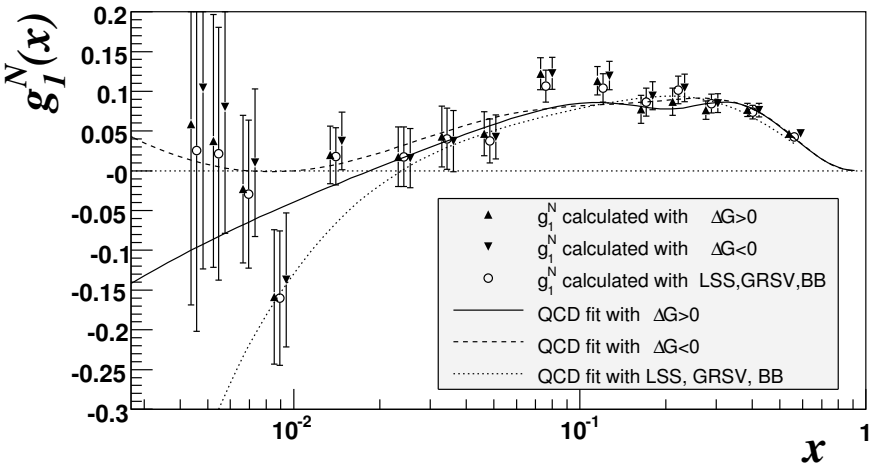

Fig. 9. The COMPASS values of g_1^N evolved to $Q^2 = 3\,(\mathrm{GeV/c})^2$. Results of QCD fits are shown by curves. In addition to our fits ($\Delta G > 0$ and $\Delta G < 0$) the curve obtained with three published parameterisations of the polarized PDF's (Blümlein and Böttcher, GRSV and LSS05 [21]) is shown. These parameterisations lead almost to the same values of $g_1^N(x_i, Q^2 = 3\,(\mathrm{GeV/c})^2)$ and have been averaged. For clarity data points evolved with different fits are shifted in x with respect to each other. Only statistical errors are shown.

In the $\overline{MS}$ scheme η_Σ is identical to the matrix element a_0, detailed below.

The direct measurement of $\Delta G/G$ [34–36], obtained at leading order in QCD, is compared with the indirect approach provided by the NLO QCD fits (Fig. 10). The unpolarised gluon distribution is taken from the MRST parametrisation [30]. The HERMES value is positive and 2σ away from zero. The measured SMC point is too imprecise to discriminate between positive or negative ΔG. The published COMPASS point, which has been obtained from a partial data sample corresponding to data collected in the years 2002 and 2003, is almost on the $\Delta G > 0$ curve, but is only 1.3σ away from the $\Delta G < 0$ one. More details and the definite results on our QCD analysis can be found at Ref. [18].

We have calculated the integral of g_1^N using exclusively the experimental values of COMPASS evolved to $\mathrm{Q_0^2} = 3\,(\mathrm{GeV/c})^2$ and averaged over the two fits. Taking into account the contributions from the fits in the unmeasured regions of $x < 0.003$ and $x > 0.7$ we obtain:

$$\Gamma_1^N \left(Q^2 = 3\,(\mathrm{GeV/c})^2\right) = 0.050 \pm 0.003(\mathrm{stat.}) \pm 0.002(\mathrm{evol.}) \pm 0.005(\mathrm{syst.})\,. \quad (12)$$

The second error accounts for the difference in Q^2 evolution between the two fits. The systematic error is the dominant one and mainly corresponds to the uncertainty on the beam and target polarisations and on the dilution factor, detailed in section 3. One should notice that, taking into account only COMPASS data, the unmeasured regions contribute only with 2 % to the integral of g_1^N.

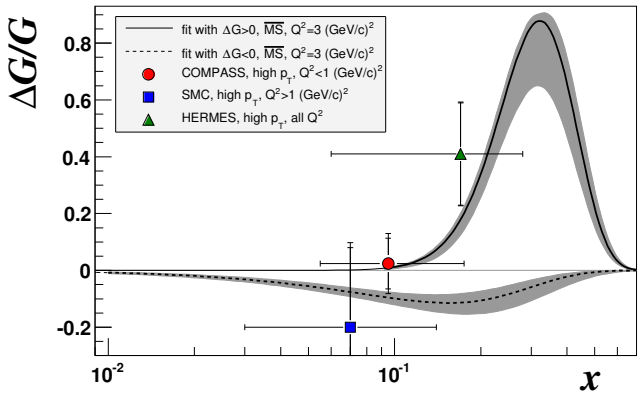

Fig. 10. Distribution of the gluon polarisation $\Delta G(x)/G(x)$ at $\mathrm{Q}^2 = 3\,(\mathrm{GeV/c})^2$ for the fits with $\Delta G > 0$ and $\Delta G < 0$ obtained with the program of Ref. [31]. The three data points show the measured values from SMC [34], HERMES [35] and COMPASS [36]. The error bars associated to the points are statistical. The error bands correspond to the statistical error on $\Delta G(x)$ at a given x. The horizontal bar on each point shows the x-range of measurement.

Γ_1^N is related to the matrix element of the singlet axial current a_0, which measures the quark spin contribution to the nucleon spin. At NLO, the relation between Γ_1^N and a_0 in the limit $Q^2 \to \infty$ ([37]) is

$$\Gamma_1^N(Q^2) = \frac{1}{9}\,\hat{C}_1^S(Q^2)\,\hat{a}_0 + \frac{1}{36}\,C_1^{\mathrm{NS}}(Q^2)\,a_8\,. \tag{13}$$

The coefficients $\hat{C}_1^S$ and C_1^{NS} have been calculated in perturbative QCD up to the third order in $\alpha_s(Q^2)$:

$$\hat{C}_1^S(Q^2) = 1 - 0.33333\Big(\frac{\alpha_s}{\pi}\Big) - 0.54959\Big(\frac{\alpha_s}{\pi}\Big)^2 - 4.44725\Big(\frac{\alpha_s}{\pi}\Big)^3\,, \tag{14}$$

$$C_1^{\mathrm{NS}}(Q^2) = 1 - \Big(\frac{\alpha_s}{\pi}\Big) - 3.5833\Big(\frac{\alpha_s}{\pi}\Big)^2 - 20.2153\Big(\frac{\alpha_s}{\pi}\Big)^3\,. \tag{15}$$

From the COMPASS result of Eq. 12 and taking the value of a_8 measured in hyperon β decay, assuming $SU(3)_f$ flavour symmetry ($a_8 = 0.585 \pm 0.025$ [20]), one obtains with the value of α_s evolved from the PDG value $\alpha_s(\mathrm{M_z}^2) = 0.1187 \pm 0.005$:

$$\hat{a}_0 = 0.33 \pm 0.03(\mathrm{stat.}) \pm 0.05(\mathrm{syst.})\,. \tag{16}$$

5 Summary

COMPASS has measured the deuteron spin asymmetry A_1^d and its longitudinal spin-dependent structure function g_1^d with improved precision at $Q^2 < 1\,(\mathrm{GeV/c})^2$ and $0.0005 < x < 0.02$, as well as $Q^2 > 1\,(\mathrm{GeV/c})^2$ and $0.004 < x < 0.7$. g_1^d is consistent with zero for $x < 0.03$. The measured values have been evolved to a common Q^2 by a NLO QCD fit of the world g_1 data. The fit yields two solutions, one corresponding to $\Delta G(x) > 0$ and other to $\Delta G(x) < 0$, which describe the data equally well. Although the shapes of the distributions are very different, their absolute values of the first moment of $\Delta G(x)$ are similar and not larger than 0.3. Taking into account only COMPASS data, the first moment Γ_1^N has been evaluated at $Q^2 = 3\,(\mathrm{GeV/c})^2$ with a statistical error of about 6 %. From this integral the matrix element of the singlet axial current $\hat{a}_0$ in the limit $Q^2 \to \infty$ is extracted. At the order α_s^3 it has been found $\hat{a}_0 = 0.33 \pm 0.03(\mathrm{stat.}) \pm 0.05(\mathrm{syst.})$.

This work was partially supported by Fundação para a Ciência e a Tecnologia – Portugal.

References

[1] M. J. Alguard et al. [E80 Coll.]: Phys. Rev. Lett. **37** (1976) 1261.

[2] J. R. Ellis and R. L. Jaffe: Phys. Rev. D **9** (1974) 1444.

[3] J. Ashman et al. [EMC Coll.]: Phys. Lett. **B206** (1988) 364.

[4] B. Adeva et al. [SMC Coll.]: Phys. Rev. D **58** (1998) 112001.

[5] P. L. Anthony et al. [E142 Coll.]: Phys. Rev. D **54** (1996) 6620.

[6] K. Abe et al. [E143 Coll.]: Phys. Rev. D **58** (1998) 112003.

[7] K. Abe et al. [E154 Coll.]: Phys. Lett. B **405** (1997) 180.

[8] P. L. Anthony et al. [E155 Coll.]: Phys. Lett. B **463** (1999) 339.

[9] A. Airapetian et al. [HERMES Coll.]: Phys. Lett. B **442** (1998) 484.

[10] X. Zheng et al. [JLAB/Hall A Coll.]: Phys. Rev. Lett. **92** (2004) 012004.

[11] G. Baum et al. [COMPASS Coll.]: CERN/SPSLC 96-14, SPSC-P 297, (1996).

[12] COMPASS Coll.: *The COMPASS Experiment at CERN*, in preparation.

[13] P. L. Anthony et al. [E155 Coll.]: Phys. Lett. B **553** (2003) 18.

[14] I. V. Akushevich and N. M. Shumeiko: J. Phys. G **20** (1994) 513.

[15] COMPASS Coll.: *Spin asymmetry A_1^d and the spin-dependent structure function g_1^d of the deuteron at low values of x and Q^2*, in preparation.

[16] B. Adeva et al. [SMC Coll.]: Phys. Rev. D **60** (1999) 072004;
erratum *ibidim* Phys. Rev. D **62** (2000) 079902.

[17] A. Airapetian et al. [HERMES Coll.]: preprint DESY/06-142, September 21, 2006.

[18] V. Yu. Alexakhin et al. [COMPASS Coll.]: CERN-PH-EP/2006-029. *Submitted to Phys. Lett. B.*.

[19] A. Airapetian et al. [HERMES Coll.]: Phys. Rev. D **75** (2005) 012003.

[20] Y. Goto et al.: Phys. Rev. D **62** (2003) 037503.

[21] The Durham HEP Databases, http://durpdg.dur.ac.uk/HEPDATA/pdf.html.

[22] J. Blümlein and H. Böttcher: Nucl. Phys. B **636** (2002) 225.

[23] M. Glück, E. Reya, M. Stratmann and W. Vogelsang: Phys. Rev. D **63** (2001) 094005.

[24] E. Leader, A. V. Sidorov and D. B. Stamenov: Phys. Rev. D **73** (2006) 034023.

[25] P. L. Anthony et al. [E155 Coll.]: Phys. Lett. B **493** (2000) 19.

[26] J. Ashman et al. [EMC Coll.]: Nucl. Phys. **B** (1989) 328.

[27] P. L. Anthony et al. [E142 Coll.]: Phys. Rev. D **54** (1996) 6620.

[28] K. Abe et al. [E154 Coll.]: Phys. Rev. Lett. **79** (1997) 26.

[29] K. Ackerstaff et al. [HERMES Coll.]: Phys. Lett. B **404** (1997) 383.

[30] A. D. Martin, R. G. Roberts, W. J. Stirling and R. S. Thorne: Eur. Phys. J. C **4** (1998) 463.

[31] B. Adeva et al. [SMC Coll.]: Phys. Rev. D **58** (1998) 112002.

[32] A. N. Sissakian, O. Yu. Shevchenko and O. N. Ivanov: Phys. Rev. D **70** (2004) 074032.

[33] R. Machleidt et al.: Phys. Rep. **149** (1987) 1.

[34] B. Adeva et al. [SMC Coll.]: Phys. Rev. D **70** (2004) 012002.

[35] A. Airapetian et al. [HERMES Coll.]: Phys. Rev. Lett. **84** (2000) 2584.

[36] E. S. Ageev et al. [COMPASS Coll.]: Phys. Lett. B **633** (2006) 25.

[37] S. A. Larin et al.: Phys. Lett. B **404** (1997) 153.